

# In situ hydrocarbon concentrations from pressurized cores in surface sediments, Northern Gulf of Mexico

Katja U. Heeschen <sup>a,\*</sup>, Hans Jürgen Hohnberg <sup>b,1</sup>, Matthias Haeckel <sup>c,2</sup>,  
Friedrich Abegg <sup>a,3</sup>, Manuela Drews <sup>c</sup>, Gerhard Bohrmann <sup>a,4</sup>

<sup>a</sup> *Research Centre Ocean Margins, University of Bremen, Post Box 330 440, D-28334 Bremen, Germany*

<sup>b</sup> *Maritime Technology, TU-Berlin, Müller-Breslau-Str., 10623 Berlin, Germany*

<sup>c</sup> *Leibniz Institute of Marine Sciences (IFM-GEOMAR), Wischhofstr. 1-3, D-24148 Kiel, Germany*

Received 2 May 2007; received in revised form 26 July 2007; accepted 17 August 2007

Available online 31 August 2007

---

## Abstract

Two newly developed coring devices, the Multi-Autoclave-Corer and the Dynamic Autoclave Piston Corer were deployed in shallow gas hydrate-bearing sediments in the northern Gulf of Mexico during research cruise SO174 (Oct–Nov 2003). For the first time, they enable the retrieval of near-surface sediment cores under ambient pressure. This enables the determination of in situ methane concentrations and amounts of gas hydrate in sediment depths where bottom water temperature and pressure changes most strongly influence gas/hydrate relationships. At seep sites of GC185 (Bush Hill) and the newly discovered sites at GC415, we determined the volume of low-weight hydrocarbons (C<sub>1</sub> through C<sub>5</sub>) from nine pressurized cores via controlled degassing. The resulting in situ methane concentrations vary by two orders of magnitudes between 0.031 and 0.985 mol kg<sup>-1</sup> pore water below the zone of sulfate depletion. This includes dissolved, free, and hydrate-bound CH<sub>4</sub>. Combined with results from conventional cores, this establishes a variability of methane concentrations in close proximity to seep sites of five orders of magnitude. In total four out of nine pressure cores had CH<sub>4</sub> concentrations above equilibrium with gas hydrates. Two of them contain gas hydrate volumes of 15% (GC185) and 18% (GC415) of pore space. The measurements prove that the highest methane concentrations are not necessarily related to the highest advection rates. Brine advection inhibits gas hydrate stability a few centimeters below the sediment surface at the depth of anaerobic oxidation of methane and thus inhibits the storage of enhanced methane volumes. Here, computerized tomography (CT) of the pressure cores detected small amounts of free gas. This finding has major implications for methane distribution, possible consumption, and escape into the bottom water in fluid flow systems related to halokinesis. © 2007 Elsevier B.V. All rights reserved.

*Keywords:* Seafloor sampling; Pressure vessel; Methane; Gas hydrates; Salinity effects; Seep; Regional index term: USA; Gulf of Mexico; Louisiana Slope

---

\* Corresponding author. Now at: National Oceanography Centre Southampton, European Way, Southampton, UK, SO14 3ZH. Tel.: +44 23 80596550; fax: +44 23 80596554.

*E-mail addresses:* [kyh@noc.soton.ac.uk](mailto:kyh@noc.soton.ac.uk) (K.U. Heeschen), [hohnberg@uni-bremen.de](mailto:hohnberg@uni-bremen.de) (H.J. Hohnberg), [mhaeckel@ifm-geomar.de](mailto:mhaeckel@ifm-geomar.de) (M. Haeckel), [abegg@uni-bremen.de](mailto:abegg@uni-bremen.de) (F. Abegg), [gbohrmann@uni-bremen.de](mailto:gbohrmann@uni-bremen.de) (G. Bohrmann).

<sup>1</sup> Now at: Research Centre Ocean Margins, University of Bremen, Post Box 330 440, D-28334 Bremen, Germany. Tel.: +49 421 218 8935; fax: +49 421 218 8664.

<sup>2</sup> Tel.: +49 431 600 2123; fax: +49 431 600 2928.

<sup>3</sup> Tel.: +49 421 218 8935; fax: +49 421 218 8664.

<sup>4</sup> Tel.: +49 421 218 8939; fax: +49 421 218 8664.

## 1. Introduction

Marine sediments along continental margins host large amounts of methane ( $C_1=CH_4$ ), a natural fuel and greenhouse gas, mainly stored in gas hydrates (Reeburgh, 2003; Archer and Buffett, 2005). The current estimates of  $CH_4$  stored within gas hydrates vary between as much as  $3 \cdot 10^{15}$  to  $115 \cdot 10^{15}$   $m^3$  methane (STP) (Kvenvolden, 1999; Milkov, 2004; Buffett and Archer, 2004). The high uncertainty of methane volumes is due to the difficulties in directly measuring the amounts of gas hydrates and free gas, because up to 99% of the methane can be lost during the recovery and sampling of gassy sediments with conventional cores (Dickens et al., 1997; Paull and Ussler, 2001). Furthermore, conventional coring cannot distinguish between free and hydrate-bound gas. Therefore, a primary goal of several ongoing research programs is to more accurately determine the local and regional inventories of methane that is stored as free, dissolved, or gas hydrate-bound methane and how this might change with time (Dickens, 2001; Judd, 2002; Milkov, 2004). This quantification of small and large scale changes of  $CH_4$  concentrations and the phase distributions of  $CH_4$  are critical for a better understanding of fluid flow systems and their dynamics in order to assess shallow gas hydrates as a future energy resource or as an environmental hazard in terms of climate change and slope stability (Kvenvolden, 1993, 1999; Sloan, 2003). From a biological point of view the in situ values are essential to determine microbial turnovers in the field (Krüger et al., 2005) and the availability of methane to microorganisms. In the past, conventional coring has already shown high regional and local variability of methane concentrations and gas hydrate distributions in shallow sediments at seep sites along active and passive margins (e.g., Ginsburg et al., 1999; Sahling et al., 2002; Joye et al., 2004; Stadnitskaia et al., 2006).

In marine sediments, under high pressure (P) and low temperature (T), methane is predominantly stored and condensed in gas hydrates if methane concentrations exceed solubility (Kvenvolden, 1988, 1993; Sloan, 1998, 2003). It forms structure I (sI) or structure II (sII) gas hydrate depending on the P–T conditions and the abundance of low-weight alkanes ( $C_2$  through  $iC_4$ ) and other gases (Sloan, 1998). Outside the gas hydrate stability zone (GHSZ) oversaturated  $CH_4$  is present as free gas (Bangs et al., 1993; Holbrook et al., 1996). Recent literature, however, indicates that free gas can also occur within the P–T stability field of gas hydrates (Abegg et al., 2003; Milkov et al., 2003, 2004) if water is absent (Suess et al., 1999; Haeckel et al., 2004) or the concentration of dissolved ions – a natural inhibitor of gas

hydrate formation – is too high (Sloan, 1998; Milkov et al., 2004). High chlorinity and local heat flow anomalies inhibit gas hydrate formation at various seep sites in the northern Gulf of Mexico (Ruppel et al., 2005; Paull et al., 2005), but the relative importance of these factors on the amount, distribution, and availability of methane was unknown prior to this study.

So far, in situ methane measurements have been unique to ODP sampling (Kvenvolden et al., 1983; Paull et al., 1996; Dickens et al., 1997, 2000; Tréhu et al., 2003, 2004; Milkov et al., 2003). The cores have manifested the high variability of gas hydrate volumes with depth (Milkov et al., 2003; Dickens et al., 1997) and the presence of free gas co-occurring with gas hydrates (Abegg et al., 2003; Milkov et al., 2003, 2004). ODP drilling, however, is not suitable for investigations of the highly variable lateral changes in methane concentration and distribution in the shallow sediments of seep sites. Therefore, new pressure-coring tools for shallow sediments were developed within the German BMBF projects OMEGA and METRO.

Here we present the first results from sampling shallow sediments with the new pressure-coring tools (MAC and DAPC, Fig. 1) that we deployed at seep sites in the northern Gulf of Mexico. The first objective of this work was to derive in situ methane concentrations in the shallow sediments at the seep sites and determine their variability. The second objective was to directly test whether free and hydrate-bound methane co-exist in the surface sediments around flow conduits and to investigate their effect on the methane concentrations closest to the seabed. Pressure tools are the only method to determine concentration differences above solubility.

## 2. Site description

This study focuses on shallow gas hydrate-bearing sediments around seeps in Green Canyon blocks GC415 and GC185 ('Bush Hill') in the northern Gulf of Mexico (GoM). In the GoM the rapid deposition of siliciclastic sediments results in a thick sedimentary succession on the continental margin. It covers Early Jurassic salt sheets (Humphris, 1979; Worrall and Snelson, 1989) that are mobile and create a submarine landscape of sub-circular to elongate basins and salt ridges (Weimer et al., 1998; Rowan et al., 1999). Halokinesis-related faults serve as efficient migration paths for hydrocarbons and brines to shallower reservoirs and the seafloor where they form numerous localized seeps expelling cold fluids free gas, and oil, resulting in gas hydrate formation (Brooks et al., 1984; Kennicutt et al., 1988; Fu and Aharon, 1998; Roberts and Carney, 1997; Sassen et al., 1999; MacDonald et al., 2003; Sager et al., 2003). Numerous seep

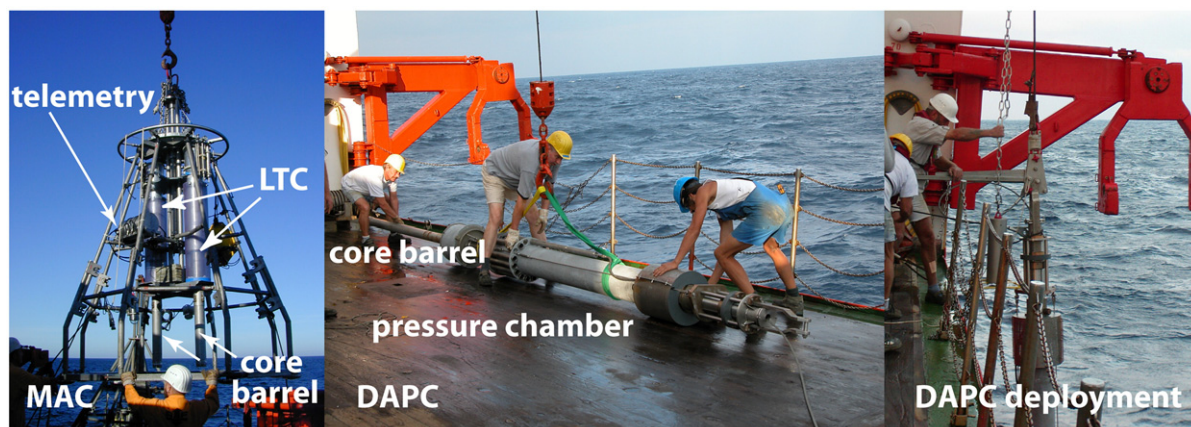


Fig. 1. The new pressure core samplers deployed during RV SONNE cruise SO174 in the Gulf of Mexico: The Multi-Autoclave-Corer (MAC) is equipped with up to four Laboratory Core Devices (LTCs) that recover cores of a maximum length of 55 cm and can be deployed with the aid of a video system (left). The Dynamic Autoclave Piston Corer (DAPC) consists of a core liner and a pressure chamber (middle) and works like a piston corer (right). It was first deployed during SO174.

locations along ridges are mainly associated with methane originating from thermocatalytic processes (thermogenic methane), whereas microbial methane from organic matter decay is the main source of minor seeps within the basins (Bernard et al., 1976; Martens et al., 1991; Thompson, 1996; Sassen et al., 1999). Ethane ( $C_2$ ) and other low-weight hydrocarbons ( $C_{2+}$ ) are mainly associated with thermogenic methane and are believed to be catagenic products formed at depth at 75 to 140 °C (Mango, 1997). Gas hydrate structures I and II have been found in the northern Gulf of Mexico (Brooks et al., 1984; Sassen et al., 1999).

Bush Hill (from here on called GC185) is located at 550 m water depth, has an area of 500 m<sup>2</sup> and is characterized by hydrate mounds covered with 10 to 30 cm of hemipelagic mud (e.g., Roberts and Aharon, 1994; Sassen et al., 1994; Reilly et al., 1996; MacDonald et al., 2003). The oil-stained sediments contain high amounts of sII gas hydrates and host a

large chemosynthetic community (Brooks et al., 1984; Sassen et al., 1999; MacDonald et al., 2003). Free natural gas discharges along a north–south striking normal fault over a salt-supported anticline (MacDonald et al., 1989).

Strong oil and gas venting also characterizes the newly discovered gas hydrate-bearing seep sites in block GC415 at 1000 m water depth. The sites were located during SO174 from known oil-slicks at the sea surface (MacDonald et al., 1996), by acoustic imaging of several gas plumes in the water column, and via chemoautotrophic communities at the seafloor (Bohrmann and Schenck, 2004). Pore water profiles established during the cruise indicate strong fluid migration (Reitz et al., 2007). The two main seep locations are at water depths of 950 m (GC415 west) and 1050 m (GC415 east) and host large amounts of gas hydrates. Despite the short distance between them, the ascending fluids have clearly different sources (Reitz et al., 2007).

Table 1

Stations and samples of pressure core devices on SO174 presenting the number of gas samples taken during degassing (gas samples), the water depth (depth), the analysis of pore water (PW) and hydrocarbon gases (HC) on sediment samples after degassing, and the recovery pressure (pressure)

Station	Device	Location	Latitude °N	Longitude °W	Depth/m	Gas samples	HC/PW analysis	Pressure, bar
63	MAC-04	GC415	27:32.530	90:59.595	1049	14	PW	75
90	DAPC-01	GC185	27:46.948	91:30.482	549	11	PW	44
97	MAC-06	GC415	27:32.588	90:59.564	1046	non	non	65
118	MAC-07	GC185	27:46.696	91:30.429	552	7	PW+HC	45
152	MAC-09	GC415	27:32.609	90:59.535	1041	5	PW	47
153	DAPC-03	GC415	27:32.600	90:59.560	1041	3	PW+HC	70
158	MAC-10	GC185	27:46.968	91:30.469	555	3	PW+HC	42
166	DAPC-04	GC415	27:33.474	90:58.855	953	3	PW+HC	70
170	MAC-12	GC415	27:33.452	90:58.866	946	1	non	115

### 3. Methods

The two autoclave tools (Fig. 1), Multi-Autoclave-Corer (MAC) and Dynamic Autoclave Piston Corer (DAPC), were constructed at the TU Berlin within the framework of the OMEGA project (Abegg et al., under revision; [http://www.tu-berlin.de/fb10/MAT/maritime\\_technology/intro/index.htm](http://www.tu-berlin.de/fb10/MAT/maritime_technology/intro/index.htm) cited March 2007) and deployed during the SO174 expedition with R/V SONNE in the Gulf of Mexico (October–November 2003). In total, we

analyzed six MAC and three DAPC cores for their hydrocarbon gas volumes and seven out of nine cores for their pore water compositions (Table 1, Fig. 2). The complete pore water data set of SO174 is published and discussed in Reitz et al. (2007).

#### 3.1. Autoclave tools

The MAC can simultaneously retrieve two to four surface sediment cores of up to 55 cm length. It is deployed using a

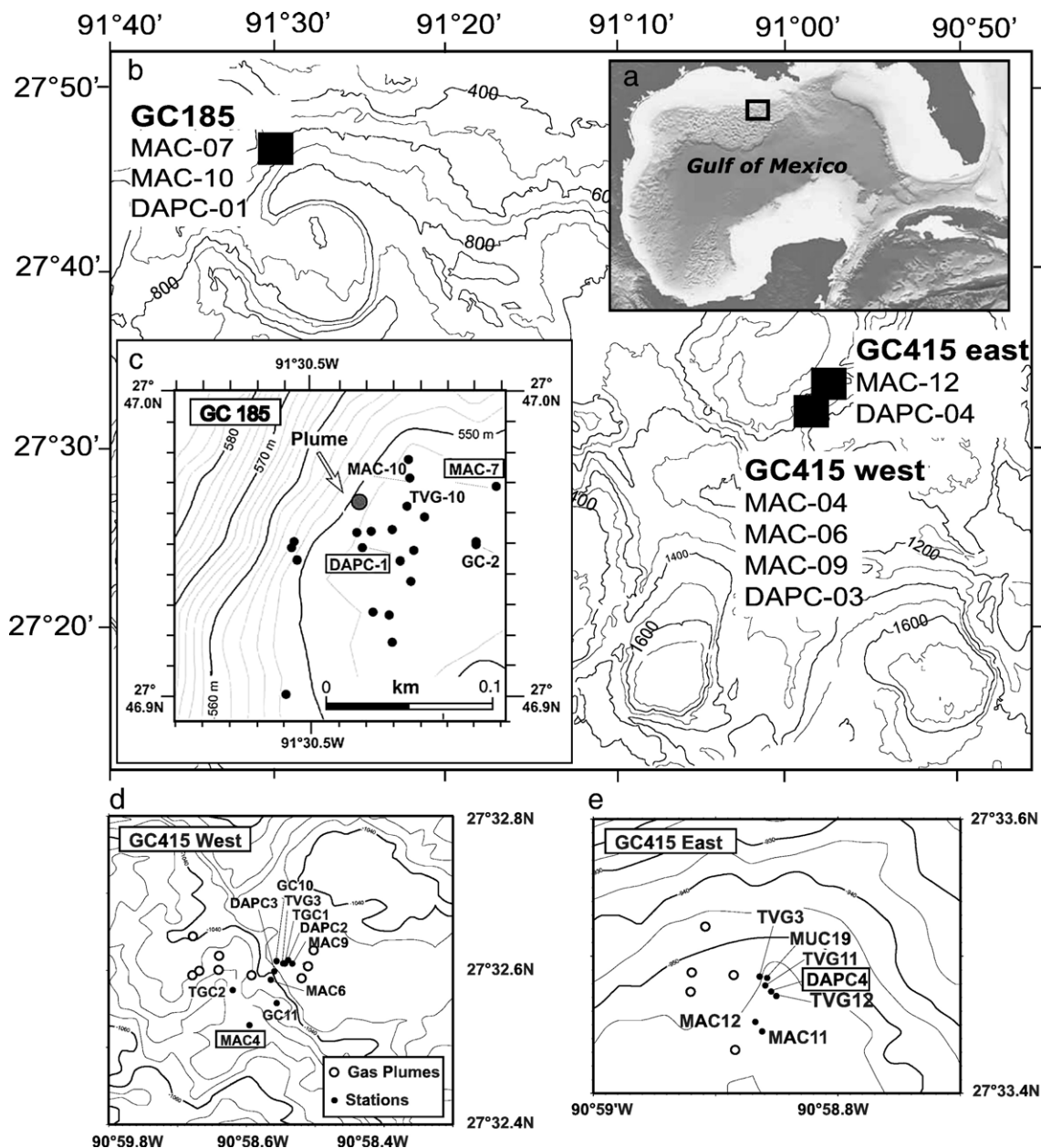


Fig. 2. Working areas in the northern Gulf of Mexico (a, b) including GC185 (c), GC415 west (d) and GC415 east (e). The detailed maps show the positions (dots) of the successful pressure core deployments (MAC and DAPC) and the positions of conventional cores. The latter are labelled if they are mentioned in the text. Stations of pressure cores with excess methane have an outside border.

video system for precise positioning. At the seafloor, each of the recovered cores is immediately pulled into a pressure chamber (LTC, Laboratory Transfer Chamber). A transparent mantle tube encloses each LTC. Once onboard, these tubes can be filled with ice or water to preserve the core temperature. The DAPC was designed to take one sediment core of up to 2.3 m in length that is then stored in a pressure chamber. The device resembles a piston core and can be released from variable heights (1–5 m above the seafloor) to enter the seafloor in free fall. The short cutting pipe is particularly suitable for sampling gas hydrate-bearing sediments. The inner radius of the core liners are 5.0 cm (MAC) and 4.2 cm (DAPC), resulting in a maximum core volume of 4.3 dm<sup>3</sup> and 12.7 dm<sup>3</sup>, respectively. The instruments can recover sediment cores at in situ pressure in water depths of up to 1400 m (MAC) and 3000 m (DAPC). A pressure-preserving system (accumulator) attached to the LTCs and the DAPC enables pressure preservation over several weeks. The design of both instruments allows X-ray Computer Tomography (CT) under in situ conditions without having to extract the core. For a detailed description of the tools see [Abegg et al. \(under revision\)](#).

### 3.2. Degassing

The handling of the pressure cores after recovery was adapted from degassing experiments of PCS cores on ODP Legs 164 and 204 ([Paull et al., 1996](#); [Dickens et al., 2000](#); [Tréhu et al., 2003](#); [Milkov et al., 2004](#)). After core recovery, the pressure chamber of the MAC or DAPC was linked to a gas tight series of Swagelok® valves ('gas manifold'). This system connects the pressure chamber to a pressure sensor (0–200 bar) for continuous recording of pressure changes, a 3-port valve for gas sub-sampling, and a 'gas catcher' ([Fig. 3](#)). The latter is a volumetric plastic cylinder inverted in a brine solution. In the cylinder, a pipe conducts the gas into the headspace above the solution such that the increasing gas volume can be read off manually. Gas sub-samples were taken during the degassing.

Unlike in earlier systems, the 3-port valve for sub-sampling is located before the cylinder to avoid further air contamination or sampling of gas mixtures. The sampled volume was added to the volume collected in the cylinder.

The degassing of MAC pressure chambers (LTC) were carried out in the onboard laboratory. Initially, a layer of cool-packs was attached to the LTC to keep the temperature reasonably stable and close to in situ temperatures during the main degassing phase. The DAPC was degassed at night on the working deck at temperatures of 24 °C ± 1 °C. The core lay on deck with its top raised. The main degassing took up several hours and was stopped when gas bubbling had ceased for several minutes. After 5 to 8 h, we reopened the valves of the DAPC or LTC to allow the release of residual gas that had accumulated due to warming of the cores to ambient temperature.

Possible sources and sinks for methane during degassing stem from bottom water enclosed in the pressure chamber surrounding the core liner. Ideally, the gas is released from the core through a valve at the top of the instrument that is connected to a hole in the piston at the top of the pressure chamber. Thus, the pathway through the water is very short. The likely exception is DAPC-04. Sediments clogged the upper pathway during the piston, leading to a significant amount of water being released until the expanding gas escaped at the bottom of the sediment core and rose through the water until reaching the open top valve.

The enclosed bottom water volumes are 10 l and 12 l for DAPC and LTC, respectively. The maximum methane concentration observed in the bottom water was <0.5 µmol/l, which is far below saturation at atmospheric pressure. The amounts of CH<sub>4</sub> that could possibly dissolve in the enclosed water volumes at atmospheric pressure are as low as 0.028 l and 0.034 l, respectively (after [Tishchenko et al., 2005](#)). Methane oxidation and production are too small to be detected with the degassing method ([Orcutt et al., 2005](#)). The accuracy of the reading from the graduated scale for gas and water is in the range of ±20 ml. For quantitative interpretations we only

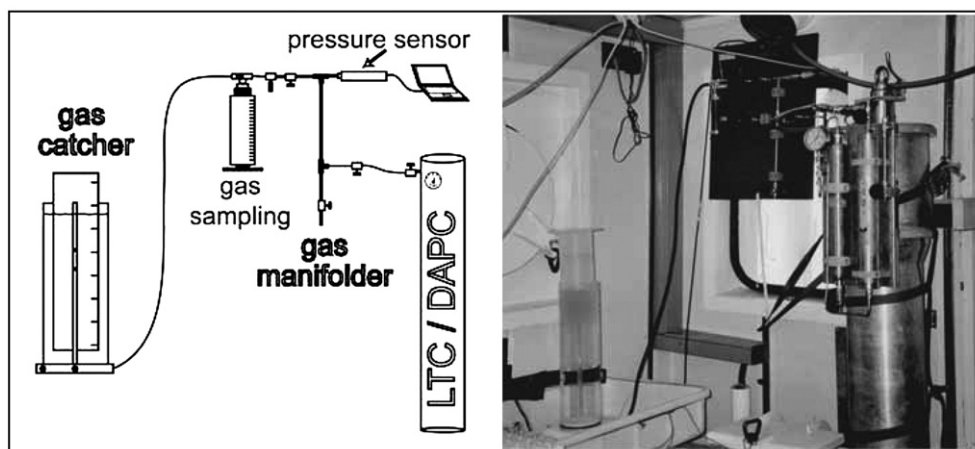


Fig. 3. Sketch and photo of degassing setup used on the MAC pressure chamber (LTC) during SO174.

consider cores with gas releases >0.5 l such that the error is <10%. The air volume initially present in the gas manifold (0.1 l) is subtracted.

Gas sub-samples were taken with a gas-tight syringe (25–50 ml) and injected into evacuated headspace vials (5 ml). A Thermo-Electron gas chromatograph was used to analyze C<sub>1</sub> through C<sub>5</sub>. It was equipped with a capillary column (Alltech: AT-Q 30 m·0.32 mm ID) and a flame ionization detector (FID). The bottled Scotty® standards were i) 1% methane (±5%) and ii) 1000 ppm C<sub>1</sub> to nC<sub>6</sub> (±5%) in helium. The relative precision of the instrument was 6% for both standards. The relative precision of up to four parallel sub-samples varied between 4 and 11% (with the exception of obviously air-contaminated samples). The sub-sample with the highest concentration was chosen for separate CH<sub>4</sub> measurements.

### 3.3. Pore water analysis

Given significant degassing, the sediment cores were extruded and sampled for pore water analysis by squeezing of the sediments. Despite the degassing, the pore water profiles are comparable to those gained from conventional cores (Reitz et al., 2007). Here, we present profiles of chloride, sulfate and sulfide from the pressure cores. CH<sub>4</sub> concentrations in pore waters were determined on twelve conventional cores (gravity cores and multi cores). Analyses were carried out using standard methods as described in Bohrmann and Schenck (2004), Reitz et al. (2007), and [http://www.geomar.de/zd/labs/labore\\_umwelt/Meth\\_englisch.html](http://www.geomar.de/zd/labs/labore_umwelt/Meth_englisch.html), cited July07).

### 3.4. X-ray computerized tomography (CT)

On SO174 Leg 2, the LTCs including the sediment cores were scanned by Computer Tomography (CT) to determine the volume and distribution of free gas and/or gas hydrate in sediments under in situ pressure. The CT-Scan shows minute variations of density and allows the distinction between gas hydrates, sediment and free gas (Abegg et al., 2003, under revision). Free gas, in particular, can be determined even in very small volumes due to its high density contrast with the other components.

## 4. Results

### 4.1. Gas volume released from pressurized cores

Gas volumes released from the pressurized sediment cores varied between 0.04 and 14.4 l (MAC) and 1.8 to 65 l (DAPC) (Fig. 4). These volumes included released gas and small amounts of water. The latter was displaced due to the expansion of gas and was mainly encountered at the beginning of the degassing. A larger volume of water was only released from DAPC-04, related to a clogged gas pathway at the top of the core (see Section 3.2). One core each at GC185 (DAPC-01) and GC415 (MAC-04) had high gas volumes. Intermediate volumes were obtained from MAC-07 at GC185 and DAPC-03 and DAPC-04 at GC415.

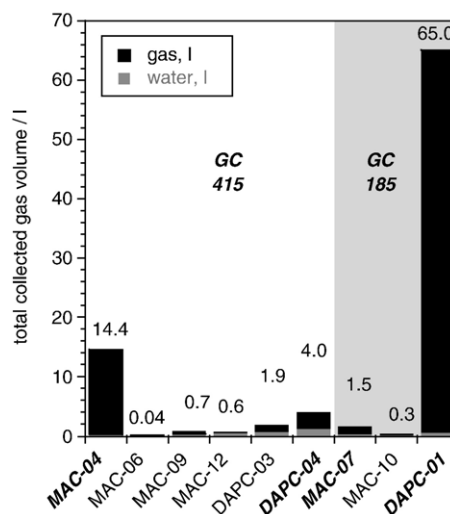


Fig. 4. Total gas volume released from the pressure cores at sampling sites GC 415, GC 185 and GC234. Total volumes are the sum of gas volume (black bars)+water volume (gray bars) — volume of gas manifold (100 ml) at STP. Cores with methane volumes exceeding volumes dissolved in the pore water are written in italic.

### 4.2. Gas composition of released gas

The average hydrocarbon compositions (Gc) of the released gas are listed in Table 2. They were calculated as follows:

$$Gc = \frac{\sum (Gc_i * (Gv_i - Gv_{i-1}))}{\sum Gv_i - Gv_{i-1}} \quad (1)$$

where Gc<sub>i</sub> is the hydrocarbon composition (%) of each sub-sample (i) and Gv<sub>i</sub> is the gas volume gained at the time the sub-sample was taken. H<sub>2</sub>S, CO<sub>2</sub>, N<sub>2</sub>, and O<sub>2</sub> were not determined in these samples. The lack of values for CO<sub>2</sub> compositions (max. 3–4%; Brooks et al., 1984) might lead to a slight overestimation of the hydrocarbon concentrations because we assume the gases to contain C<sub>1</sub>–iC<sub>5</sub> hydrocarbons only. The sum of nC<sub>5+</sub> hydrocarbon concentrations is negligible. The system is gas tight and inert gas measurements from later investigations with the DAPC showed air contaminations in the main degassing period of less than 5% (Heeschen et al., 2006). The compositions of C<sub>1</sub>–iC<sub>5</sub> are calculated in percent (%) of the total amount of low-weight alkanes C<sub>1</sub>–iC<sub>5</sub> (%  $\sum C_{1-5}$ ) to exclude concentration changes caused by air contamination during sub-sampling.

The compositions range from 82.7% to 99.7% methane, 0.3 to 3.77% ethane, and 0.1% to 9.3% propane. On average, methane compositions are considerably higher at GC415 than at GC185 and tend towards higher C<sub>1</sub>/C<sub>2+</sub> ratios in smaller gas volumes. At GC415 two cores (MAC-12 and DAPC-03) have a methane composition >99%. Cores from GC185 have C<sub>2</sub>/C<sub>3</sub> < 1, whereas at GC415 this is only true for DAPC-04. As for iC<sub>4</sub>, on average the compositions are higher at GC185 than at GC415.

Table 2  
Total gas volume released upon degassing and its hydrocarbon composition

Location	Station	Gas volume, ml	C <sub>1</sub> , %*	C <sub>2</sub> , %	C <sub>3</sub> , %	iC <sub>4</sub> , %	nC <sub>4</sub> , %	iC <sub>5</sub> , %
GC415	MAC-04	14394	94.70	3.77	0.90	0.45	0.10	0.03
	MAC-09	712	95.67	1.80	1.29	0.98	0.03	0.04
	MAC-12	520	99.29	0.47	0.16	0.08	n.d.	n.d.
	DAPC-03	1874	99.70	0.25	0.05	n.d.	n.d.	n.d.
	DAPC-04	3976	82.74	3.18	9.34	3.27	0.88	0.60
GC185	MAC-07	1545	86.08	3.28	6.02	1.94	0.31	2.01
	MAC-10	309	96.95	0.88	1.37	0.51	0.10	0.17
	DAPC-01	65000	87.76	3.10	6.72	1.91	0.37	0.03

\* Ratios of C<sub>1</sub>–iC<sub>5</sub> in relation to the total amount of C<sub>1</sub>–iC<sub>5</sub> (weighed and averaged over time).

Thus, the highest collected gas volumes – DAPC-01 and MAC-04 – show contrasting C<sub>2</sub>/C<sub>3</sub> ratios. The concentrations of nC<sub>4</sub> and iC<sub>5</sub> are low except for cores with intermediate gas volumes, MAC-07 and DAPC-04.

#### 4.3. Hydrocarbon concentrations in the pressure cores

The in situ concentrations of low-weight hydrocarbons in the pore water of the pressure cores (Table 3) are theoretical values since they exceed saturation and include dissolved, free, and hydrate-bound phases. They can be calculated from the total gas volume of each hydrocarbon (% hydrocarbon\*  $\sum Gv_i - Gv_{i-1}$ ), which is converted into mol/kg pore water based on the measured core length, pore space, the ideal gas law, and the density of salt water (Dickens et al., 1997, 2000). For these calculations, we only consider the core length below the zone of the anaerobic oxidation of methane (AOM), because only in this interval can the CH<sub>4</sub> concentrations exceed conditions to form gas hydrates. In the absence of other information we assume a uniform hydrocarbon distribution below the AOM zone. All CH<sub>4</sub> exceeding the equilibrium concentration (excess methane) in the presence of gas hydrate (C<sub>eq</sub>) forms either hydrates or free gas. Thus, subtracting C<sub>eq</sub> from the calculated in situ CH<sub>4</sub> concentration (C<sub>m</sub>) results in the amount of hydrate-bound or free methane. C<sub>eq</sub> in the presence of sI gas hydrate can be calculated using the algorithm of Tishchenko et al. (2005). C<sub>eq</sub> is 0.067 mol/kg for GC185 and 0.054 mol/kg for GC415 (Fig. 5). There is no algorithm for sII gas hydrates as yet. If there was, C<sub>eq</sub> should be slightly lower due to a greater stability of sII hydrates.

Table 3  
Molalities of C<sub>1</sub>–iC<sub>5</sub> in pore water (mol/kg pore water) below the AOM zone

Location	Station	Methane	Ethane	Propane	i-Butane	n-Butane	i-Pentane
GC415	MAC-04	0.9849	0.0392	0.0093	0.0047	0.0010	0.0003
	MAC-09	0.0592	0.0011	0.0008	0.0006	0.0000	0.0000
	MAC-12*	0.0528	0.0003	0.0001	0.0000	0.0000	0.0000
	DAPC-03	0.0308	0.0001	0.0000	0.0000	0.0000	0.0000
	DAPC-04	0.0629	0.0024	0.0071	0.0025	0.0007	0.0005
GC185	MAC-07	0.1159	0.0044	0.0081	0.0026	0.0004	0.0027
	MAC-10*	–	–	–	–	–	–
	DAPC-01	0.8572	0.0302	0.0656	0.0187	0.0036	0.0003

\* No pore water data are available for MAC-12. In 3 out of 4 MAC cores the lower limit of the AOM zone is less than 10 cm deep; the lower limit in MAC-12 is set at 10 cm. In MAC-10 the lower limit of the AOM was not reached.

In situ CH<sub>4</sub> concentrations range from 0.03 to 0.985 mol/kg. Four cores exceeded CH<sub>4</sub> saturation in the presence of gas hydrate (Fig. 5 and Table 4). By far the highest amounts of CH<sub>4</sub> and C<sub>2</sub> were found in DAPC-01 (GC185 1) and MAC-04 (GC415). C<sub>3</sub> through nC<sub>4</sub> concentrations were more variable. Two other cores with excess methane, MAC-07 (GC185) and DAPC-04 (GC415), have intermediate CH<sub>4</sub> concentrations but very high concentrations in C<sub>3+</sub>. Cores with excess CH<sub>4</sub> concentrations have the same hydrocarbon compositions at GC185 (MAC-07, DAPC-01) but differ significantly at GC415east and GC415west (DAPC-04, MAC-04). CH<sub>4</sub> concentrations below C<sub>eq</sub> in MAC-12, DAPC-03, MAC-09 and MAC-10 make any occurrence of gas hydrates unlikely. In DAPC-03 the lower boundary of the AOM zone was reached such that gas hydrate occurrence could have been possible. In MAC-10 this was not the case. No pore water data are available for MAC-06 and MAC-12.

#### 4.4. Volume–pressure relationships

Volume–pressure (V–P) relationships (Fig. 6) from the degassing of pressurized cores show specific characteristics if gas hydrates are present (Hunt, 1979; Dickens et al., 2000). Hydrate-bound gas cannot be released until a certain threshold pressure is reached, which can be predicted from the stability conditions (i.e., the temperature, salinity and gas composition). Assuming equilibrium conditions, an isobaric degassing would follow this threshold because of the continuous release of compressed gas from the decomposing gas hydrate. Under the

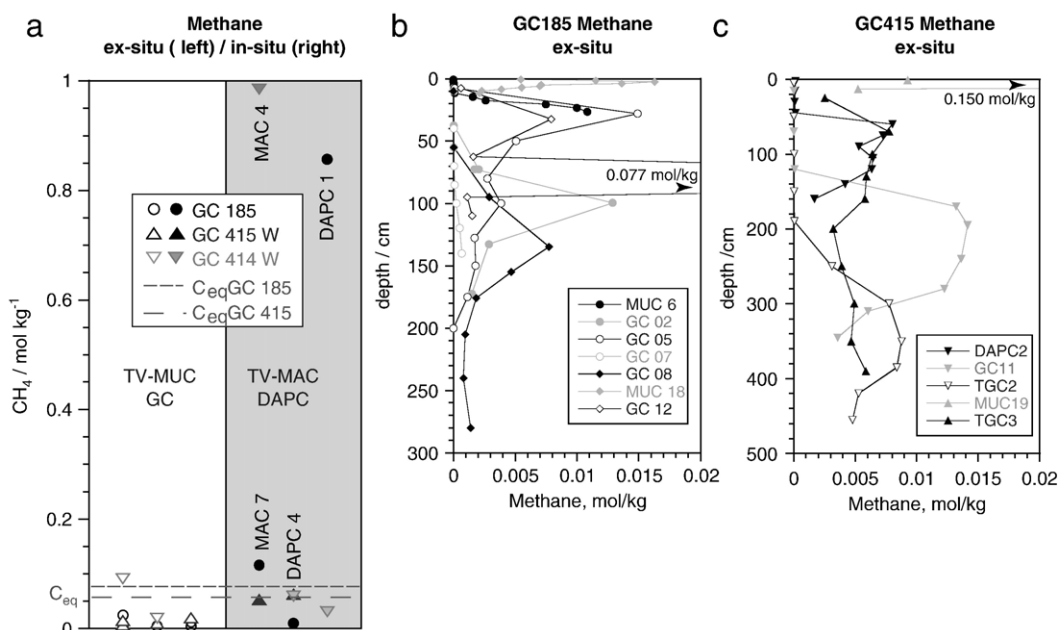


Fig. 5. a) Methane concentrations from conventional coring (open symbols) and pressurized coring (closed symbols). The dashed line marks the  $\text{CH}_4$  equilibrium concentration in the presence of gas hydrate  $C_{\text{eq}}$  (calculated after Tishchenko et al., 2005); b) methane concentration profiles from conventional (ex situ) measurements at GC185 and c) GC415 (East: upside down triangles).

non-equilibrium conditions of the degassing experiments, V–P plots from gas hydrate-bearing cores have a high threshold and show smaller gradients and a slightly convex curvature while gas hydrates dissociate below the threshold pressure. The pressure decrease following this period represents the final exsolution of the residual and dissolved gases. In theory, only this period would be associated with a pressure decrease. A concave curvature during this stage arises from the non-equilibrium conditions of the degassing due to long pathways within the core (Dickens et al., 2000). If free gas occurs in the cores, there is no threshold pressure but the gas should be released immediately (Milkov et al., 2004). However, pathways within the core can cause a short delay, and lead to the initial displacement of water

that was observed in all degassing experiments. Irregularities in degassing rates can be induced by the discontinuous and endothermic dissociation of gas hydrate, irregular pathways for free gas through the sediment, and clogged conduits.

The V–P plots of cores with the highest gas volumes, MAC-04 and DAPC-01 (Fig. 6a, b), show an onset of degassing at  $40 \pm 5$  bar and a convex curvature in the time–pressure (T–P) and V–P plots between 30 and 10 bar. The onset of degassing is immediate for DAPC-01, whereas the threshold pressure of MAC-04 is reached following a sharp drop in pressure with very little volume increase. At roughly 10 bar, the curvature in the V–P plots of both cores change gradients. A strong drop in pressure to less than 5 bar characterizes the V–P and T–P correlations of cores with

Table 4

In situ methane concentrations ( $C_m$ ), amount of dissolved methane ( $C_{\text{diss}}$ ) and gas hydrate ratios in pressure cores assuming an occurrence of methane below the AOM reaction zone

Station	$C$ , cm	$C_{\text{AOM}}$ , cm	$C_m$ , mol/kg	$C_{\text{eq}}$ , mol/kg	$C_{\text{diss}}$ , l	GH vol. *, l	GH, %ps	GH, %cv
MAC-04	15	10	0.985	0.054	0.74	0.099	18.0	13.3
MAC-09	18	9	0.059	0.054	0.61	–	–	–
MAC-12	20	10* <sup>1</sup>	0.053	0.054	0.53	–	–	–
DAPC-03	126	81	0.031	0.054	3.34	–	–	–
DAPC-04	120	75	0.063	0.054	2.78	0.004	0.2	0.2
MAC-07	18	9	0.116	0.067	0.76	0.004	1.0	0.8
MAC-10	23	0	–	0.067	–	–	–	–
DAPC-01	150	115	0.857	0.067	4.39	0.403	15.3	8.1

$C$  = Core length,  $C_{\text{AOM}}$  = core length below AOM zone, GH = gas hydrate, vol = volume, ps = pore space and cv = core volume.

\* This gas:water ratio of 132/1 is in between the ratio observed by Brooks et al. (1984) (70/1) and those of other authors: 140/1 (Milkov and Sassen, 2001); 160/1 (Chen and Cathles, 2003).

\* <sup>1</sup> No pore water data are available. In 3 out of 4 MAC cores the lower limit of the AOM zone is less than 10 cm deep.

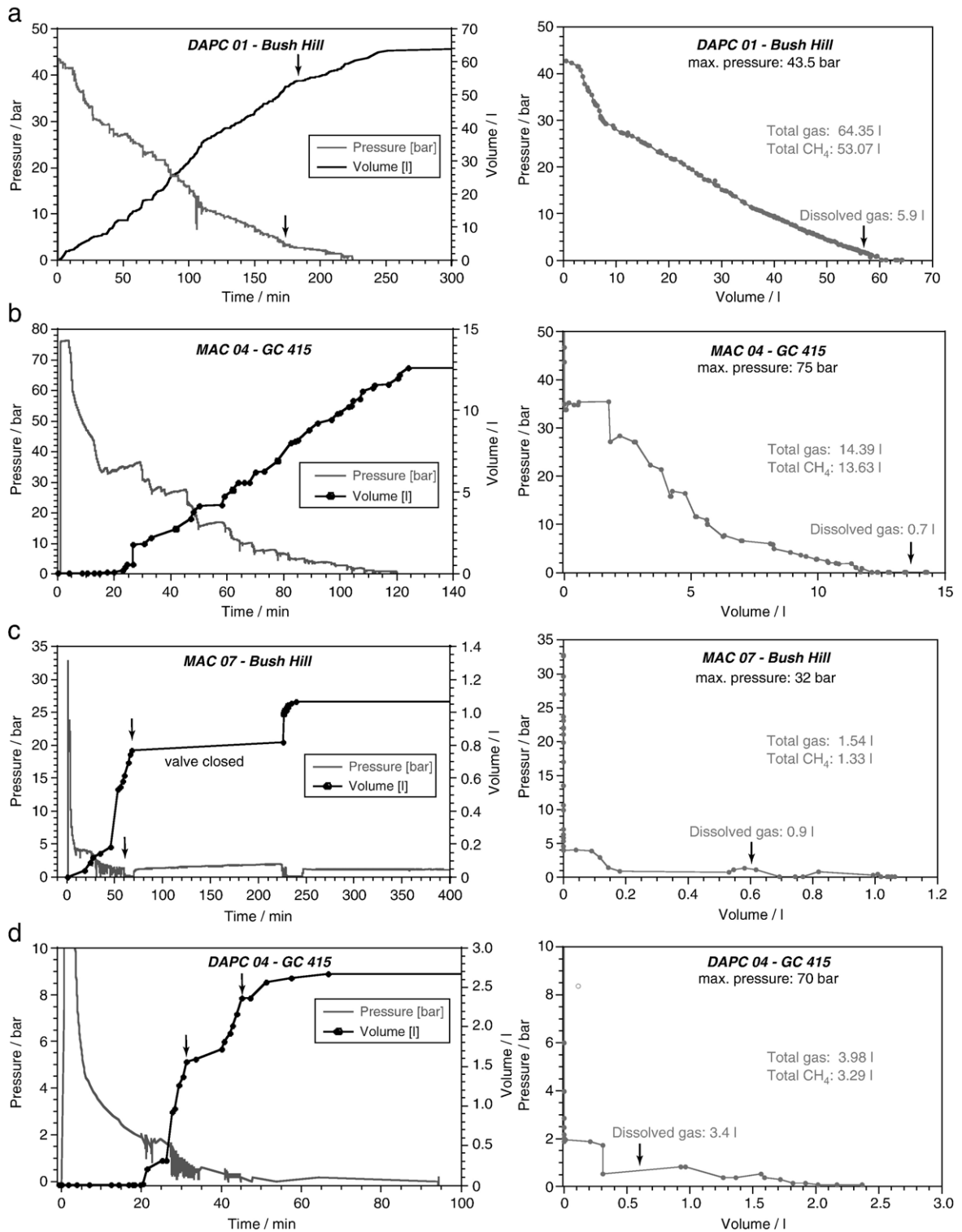


Fig. 6. Pressure–time, volume–time and pressure–volume curves of the degassing from cores with high gas volumes (a: DAPC-01, b: MAC-04) and intermediate gas volumes (c: MAC-07, d: DAPC-04). The plots do not include the released water volume and show the time of main degassing only. Note the different pressure scales. The black arrows mark the amount of dissolved gases as calculated from  $C_{eq}$  (after Tishchenko et al., 2005) and the pore water volumes below the AOM reaction zone. In MAC-04 this amount is released after the main degassing period and therefore it is not marked in the time–pressure graph.

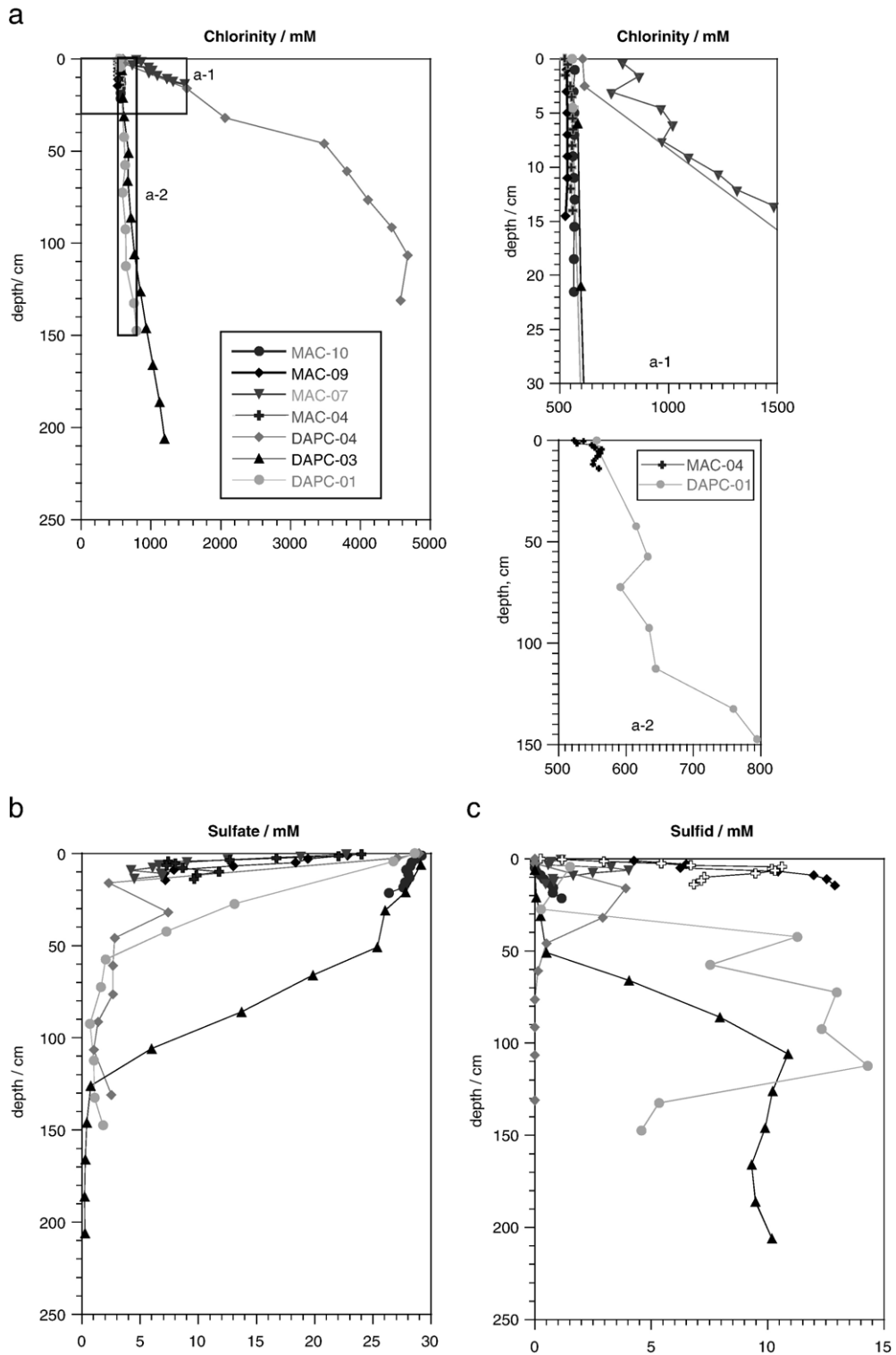


Fig. 7. a) Chloride pore water profiles from all pressure cores with detailed plots of the surface changes and the gas hydrate-containing cores DAPC-01 and MAC-04 which have irregular chloride profiles due to gas hydrate dissociation; b) pore water profiles of pressure cores of sulfate and c) sulfide.

intermediate volumes, DAPC-04 and MAC-07 (Fig. 6c, d). Most of the volume increase takes place at 1–2 bar. The gas release is very irregular and consists of short bubble eruptions with rapid pressure decrease, followed by quiet periods with little gas volume increase. Rather than ‘saw-tooth’ like degassing characteristics, the T–P correlation shows ‘needle-shaped’ peaks. There is no correlation between gradient changes in the V–P plots and the calculated amount of dissolved gas in each core (black arrows).

#### 4.5. Pore water profiles

Regardless of seep location, there are two groups of chloride profiles detected in the pressure cores (Fig. 7a). This is of major importance to the gas hydrate distribution. The cores with high gas volumes, DAPC-01 and MAC-04, belong to the group with a small increase in chloride with depth, whereas the chloride profiles of MAC-07 and DAPC-04 show a steep increase with a concave downward curvature in the case of DAPC-04. DAPC-01 and MAC-04 both show an irregular decrease in chlorinity just below the sulfate depletion depth related to gas hydrate dissociation.

The H<sub>2</sub>S and sulfate profiles indicate that, apart from MAC-10, all cores penetrated the AOM zone and that, apart from DAPC-03 the lower boundary of this zone is extremely shallow and reached within the upper 10 cm of the cores. Pore water profiles were not obtained for MAC-06 and MAC-12. However, the very small gas volumes released from these two cores might indicate that the AOM zone was not penetrated or that CH<sub>4</sub> fluxes at the sampling location were too small to supply excess methane.

#### 4.6. Gas hydrate compositions

Several gas hydrate samples were recovered during SO174, using TV-grab, gravity or multi corer (Table 5). Their C<sub>1</sub> compositions vary between 73 and 83% and the C<sub>1</sub>/C<sub>2+</sub> ratios are similar at GC185 and GC415 west but are slightly lower at GC415 east. C<sub>2</sub>/C<sub>3</sub> ratios are high and <1 on average at GC185 where they range between 1.05 (TVG-10) and 0.41 (GC-02). The C<sub>1</sub> composition at GC185 is stable.

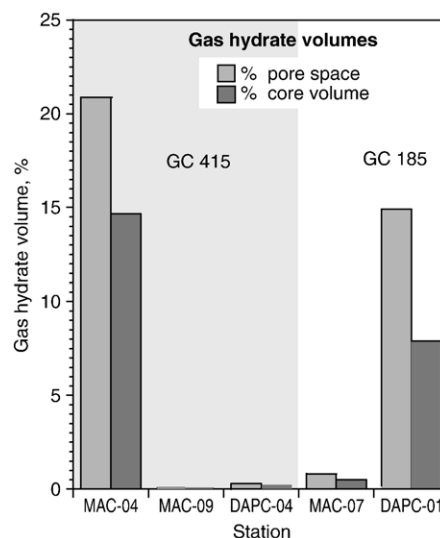


Fig. 8. Amount of gas hydrate in pressurized cores of GC415 and GC185 as a percentage of occupied pore space (dark) and percentage of core volume (light).

#### 4.7. Gas hydrate volumes

The in situ CH<sub>4</sub> concentration in the pore water ( $C_m$ ) is composed of free ( $C_g$ ) or hydrate-bound methane ( $C_{hb}$ ) and dissolved methane ( $C_{eq}$ ), thus:  $C_{hb} = C_m - C_{eq}$  or  $C_g = C_m - C_{eq}$  (Dickens et al., 1997). Our samples do not allow a resolution of small amounts of free gas coexisting with gas hydrate, which was possible for less complex sI gas hydrates (Milkov et al., 2004).  $C_{hb}$  is multiplied by the pore water volume below the AOM zone and converted into a gas hydrate volume assuming a hydration number of 6.1 (Lu and Matsumoto, 2005) and thus a cage occupancy of 90% with methane, resulting in a methane gas/water ratio of 132/1 for structure II (ideal: 182:1; Sloan, 1998) given a gas composition of approximately 78% C<sub>1</sub> and 22% C<sub>2+</sub>.

The gas hydrate volumes in the four pressure cores range between 4 and 403 cm<sup>3</sup> (Fig. 8), with the highest volumes of 105

Table 5

Averaged (avg) hydrocarbon compositions of gas hydrates sampled at GC185 and GC415 and the standard deviation (stdev) encountered in the samples (see Fig. 1 for locations)

Location	C <sub>1</sub> , %	C <sub>2</sub> , %	C <sub>3</sub> , %	iC <sub>4</sub> , %	n C <sub>4</sub> , %	iC <sub>5</sub> , %	Number of samples
GC185, avg	72.55	10.91	12.73	2.56	1.22	0.02	n = 12
stdev	1.89	2.82	2.11	1.05	0.20	0.01	
GC185, TVG-10	72.64	12.37	11.68	1.98	1.31	0.02	n = 9
stdev	2.17	1.42	1.20	0.25	0.14	0.00	
C185, GC02	72.28	6.54	15.87	4.32	0.95	0.05	n = 3
stdev	0.24	0.54	0.60	0.29	0.06	0.02	
GC415 East	83.31	7.26	6.73	1.48	1.16	0.02	n = 5
stdev	2.94	1.64	1.67	0.41	0.26	0.02	
GC415 West	77.03	12.19	7.85	1.39	2.09	0.03	n = 3
stdev	5.61	2.32	4.37	0.70	0.75	0.03	
GC185, Mean	76.3	8.1	11.6	2.7	1.0	0.0	As cited in Chen and Cathles (2003)

and 403 cm<sup>3</sup> in MAC-04 (GC415) and DAPC-01 (GC185), respectively. They amount to 13% and 8% of the core volumes (%cv) or 18% and 15% of the pore space (%ps) below the AOM reaction zone, respectively. MAC-07 has a possible gas hydrate volume of 1.0%cv and 0.8%ps. The low ratio of 0.1%ps or less than 1 ml of gas hydrate in MAC-09 is not used in the discussion since it is below the accuracy of the method. All other in situ concentrations are below  $C_{eq}$ .

## 5. Discussion

### 5.1. In situ methane concentrations

#### 5.1.1. Variations and distribution

Results presented here provide the first in situ concentrations of CH<sub>4</sub> in shallow sediments of seep sites. They exceed ex situ values (i.e., values measured on samples recovered in conventional cores) from seep sites of the Green Canyon block by two orders of magnitude when gas hydrates are present (Fig. 5). This is despite the fast recovery at shallow water depths and the immediate sampling of gravity cores from foil liners. It is noteworthy that in situ concentrations not only exceed ex situ values but also exceed theoretical equilibrium concentrations. Thus, pressure coring combined with degassing (Dickens et al., 1997) and/or CT is the only method so far that can detect true CH<sub>4</sub> concentrations and, in particular, the occurrence of excess methane in shallow sediments. It is also the only method to detect the CH<sub>4</sub> volumes from all phases, dissolved, hydrate-bound and free gas.

The variability of ex situ values at seep sites is in the range of three orders of magnitude on lateral scales of only tens of meters (Sahling et al., 2002; Joye et al., 2004). Combining our ex situ and in situ data sets (Fig. 5), the small-scale differences within the seep sites vary over three to four orders of magnitude at GC415 (5 and 985 mmol/kg) and GC185 (0.5 and 857 mmol/kg) at depth below 1 m. Differences are even greater in the uppermost 10 cm of the cores, which is related to the varying depth of the AOM zone. This clearly demonstrates the spatial variability of focused fluid flow even in the shallow sediments of seep environments, which puts strain on chemosynthetic ecosystems that have to adapt to the strong lateral gradients. In deep sediments, ODP pressure coring had observed differences of up to three orders of magnitude, although average concentrations were slightly higher, ranging between 1.9 mol/l (Milkov et al., 2003) and 3.1 mol/l (Dickens et al., 1997).

### 5.2. Excess methane in gas hydrates and free gas

Four out of nine cores have excess CH<sub>4</sub> (Fig. 5, Table 4). Assuming this CH<sub>4</sub> to be hydrate-bound, these

cores contain gas hydrate to pore water ratios between 0.2 and 18%ps. However, it was pointed out earlier that strong brine advection causes high salinities in shallow sediments at various sites in the Gulf of Mexico and that, as a consequence, gas hydrates are not stable (Paull et al., 2005; Ruppel et al., 2005). Our results confirm that only two cores, DAPC-01 (GC185) and MAC-04 (GC415), contain gas hydrate, whereas the other two cores with excess methane and high chloride concentrations, MAC-07 (GC185) and DAPC-04 (GC415), contain free gas only.

#### 5.2.1. Degassing characteristics

Only DAPC-01 and MAC-04 (Fig. 6a, b) have high gas volumes, high threshold pressures and strong gas release at high pressure. MAC-04 was recovered at 75 bar and low in situ temperature (4.5 °C) and was significantly cooled upon recovery. The threshold pressure of 35 bar coincides with the limit of stability at the core site for gas hydrates given the measured composition and a temperature of 6.6 °C (after Sloan, 1998). The convex curvature further indicates gas hydrate decomposition. In DAPC-01 gas hydrate decomposed before degassing, due to by the temperature increase on deck and a small decrease in pressure in the liner. This caused the presence of free gas in the core and its immediate release at high pressure. The linear correlation of V and P is based on the fact that methane behaves approximately like an ideal gas.

The V–P plots of the two cores with small volumes of excess methane, DAPC-04 and MAC-07 (Fig. 6c, d), have threshold pressures far below the pressure corresponding to gas hydrate stability and the plots show a range of ‘needle’-shaped pressure drops. Free gas should be released immediately, provided that the gas pressure is sufficient to form fractures that serve as conduits. Gas quickly escapes at high flow rates until pressure is too low to maintain a conduit. This process repeats as the enclosed gas expands immediately (‘needle like peaks’). Johnson et al. (2002) observed very similar time–pressure–volume behavior in bubble growth experiments associated with fracturing of soft sediment.

#### 5.2.2. Gas compositions

The composition of the released gas (Table 2) is also indicative of the existence of free gas as was shown for Hydrate Ridge and gas hydrate sl occurrences using C<sub>3</sub> (Milkov et al., 2004). In comparison to other cores, DAPC-04 and MAC-07 have higher percentages of nC<sub>4</sub> and iC<sub>5</sub> in the released gas volumes, but neither of these alkanes serves as a major guest molecule in sII gas

hydrates (Sloan, 1998). At GC185, the average  $iC_5$  composition of the seep and reservoir gas is known to be about 0.2 vol.% (Sassen et al., 2001) and thus much smaller than the gas collected from MAC-07. The accumulation of  $iC_5$  in pore water and gas voids in the sediment may well relate to its continuous exclusion from gas hydrate formation and reduced biodegradation of these higher alkanes (James and Burns, 1984; Sassen et al., 2001).

### 5.2.3. Proof of free gas via CT-imaging

Proof of free gas in sediment cores is hard to obtain because gas escapes during the recovery of conventional cores and decomposing gas hydrates form secondary bubbles. In contrast, computerized X-ray tomography (CT) can visualize the constituents of sediment cores recovered in the new pressure tools (Fig. 9) (Abegg et al., 2003, under revision). The medical CT on board SO174 was used to scan the sediment cores within the LTCs, including MAC-07. Here the CT-images show the clear presence of gas voids (Fig. 9). The depth range of gas abundance in the core is 12.5–14.8 cm, where gas voids reached a maximum of up to 1.5%cv. The total amount of gas in this layer equals 1.9 ml of gas at in situ pressure.

We can compare the results from the degassing method with those of the CT scan if we assume all excess methane from the degassing of MAC-07 to be present as free gas in the depth range of 12.5–14.8 cm.

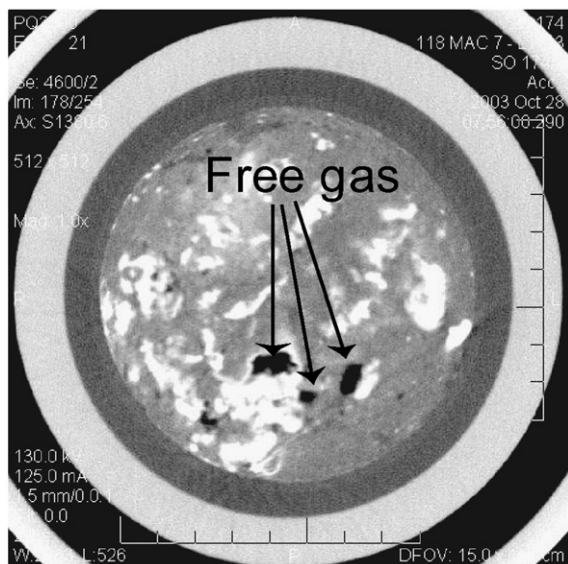


Fig. 9. a) Computer tomography (CT) image of a sediment slice from MAC-07 showing gas voids (black) within the sediment matrix (gray) and carbonates (white).

Degassing results in a gas content of 5%cv or 22 ml at 5.4 MPa compared to 1.5%cv calculated from the CT scan. One likely explanation for at least part of this discrepancy is the resolution of the mobile CT, which was  $0.13 \text{ mm}^3/\text{voxel}$ , such that gas bubbles smaller than 0.3 mm in diameter or 0.004 ml at 5.4 MPa cannot be detected. It takes only 260 bubbles of this very small size to form 1 ml of gas at in situ pressure.

### 5.3. Brine advection reduces the GHSZ in 'thermogenic' gas provinces

Assuming seawater salinity, the occurrence of only free gas is unexpected given that pressure and temperature conditions should allow gas hydrate formation. However, at high salinity, the gas hydrate stability zone (GHSZ) can become significantly shallower, as reported from other seep provinces in the Gulf of Mexico where strong advection of saline fluids originating from fossil salt deposits occurs (Martens et al., 1991; Paull et al., 2005; Ruppel et al., 2005).

The pore water profiles down cores MAC-07 and DAPC-04 have high chloride concentrations, suggesting that the GHSZ shoals significantly in these cores (Fig. 7a). The chloride profiles have a prominent concave downward curvature that indicates strong advection of saline fluids (Bernard, 1979; Ruppel et al., 2005). In both cores the chloride concentration is high enough to inhibit gas hydrate formation a few centimeters below the seafloor (shown for MAC-07, Fig. 10). At the measured in situ bottom water temperature of  $9.1 \text{ }^\circ\text{C}$  (S. Sommer, IFM-GEOMAR, Kiel, personal communication, 2005), the known gas hydrate composition and the present chloride concentrations, the lower boundary of the GHSZ in MAC-07 is located at 6–10 cm below seafloor (Fig. 10b). Thus, gas hydrates would only be stable above this depth whereas excess methane is present as free gas below. In core DAPC-04 the corresponding depth is 46 cm below the seafloor, given a present in situ temperature of  $5.42 \text{ }^\circ\text{C}$  (W. Brückmann, IFM-GEOMAR, personal communication, 2005) and a salt content of 22 wt.%. In contrast, gas hydrate is stable throughout the depths of cores DAPC-01 and MAC-04, both of which had gas hydrates and comparably low chloride increase with depth. Cores DAPC-01 and MAC-07 at GC185 are less than 100 m apart. This shows how important the pore water composition is in controlling the lateral variation in gas hydrate concentration. Equally important are changes in the gas composition as shown from the different stability curves of the gas hydrates present (TVG 10 and GC 2 Fig. 10).

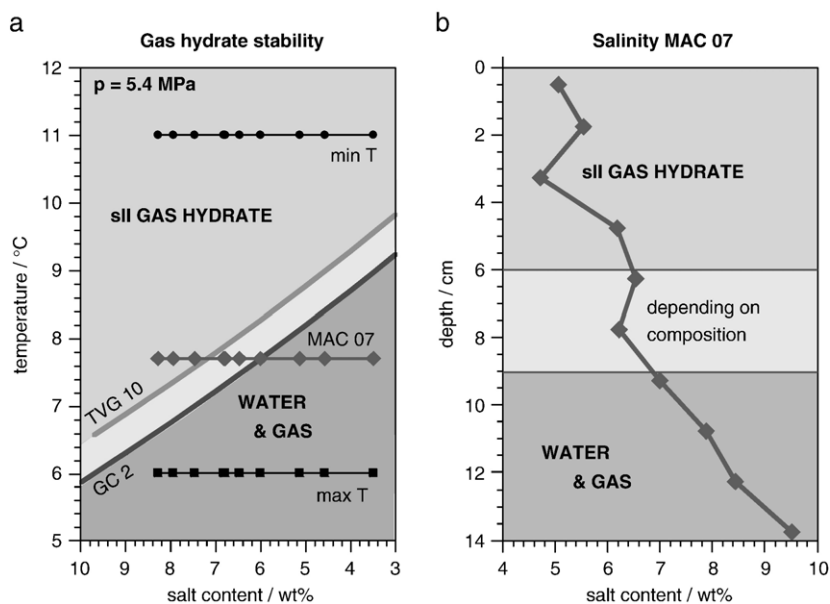


Fig. 10. a) Stability of sII gas hydrate as a function of temperature and salinity for a constant pressure of 5.4 MPa (pressure at GC185) (calculated with CSMHYD program, Sloan, 1998). The compositions of the sII gas hydrates are taken from GC-02 and TVG-10 sampled on SO174 at GC185 (Table 5). The bottom water temperature at GC185 varies between 6 and 11 °C (MacDonald et al., 1994). The temperature measured on SO174 was 9.4 °C. b) Derived occurrence of sII gas hydrate and free gas in MAC-07 based on the salinity-depth diagram of the core MAC-07. The input variables for the hydrate-bound gases in the CSMHYD program were derived to match the compositions of GC-02 and TVG-10 gas hydrates:  $C_1=94.45$ ,  $C_2=4.4$ ,  $C_3=0.68$ ,  $iC_4=0.14$ ,  $nC_4=0.32$ , and  $iC_5=0.01$  (GC-02) and  $C_1=91.26$ ,  $C_2=7.78$ ,  $C_3=0.47$ ,  $iC_4=0.06$ ,  $nC_4=0.41$ , and  $iC_5=0.02$  (TVG-10).

#### 5.4. Spatial variability of methane in relation to fluid flow

In MAC-07 and DAPC-04, the lower boundary of the GHSZ is above the depth of the AOM reaction zone which is located at  $\sim 10$  cm in MAC-07 and  $\sim 50$  cm in DAPC-04 (Figs. 6b, c and 10). However, above the AOM zone,  $CH_4$  concentrations are too low for gas hydrate formation (Iversen and Jørgensen, 1985) and thus no gas hydrate forms at these sites. This is despite the fact that these areas have very high advection rates of methane-rich fluids and are assumed to have the highest  $CH_4$  concentrations. However, compared to hydrate-containing cores, in situ  $CH_4$  concentrations were one order of magnitude lower where they coincide with brine advection and excess  $CH_4$  occurrence is restricted to the free gas phase. Free gas is less compressed than hydrate-bound gas, such that similar volumes contain less gas. The free gas also quickly escapes from the top sediment layers into the water column due to its low density and the low sediment compaction. Consequently, this methane is less accessible for microbial oxidation and the transport of methane from the sediment is enhanced. As with increasing salinity due to brine advection, high heat flow rates reduce the GHSZ as also observed in the GoM (Ruppel et al., 2005) and, for example, at Håkon Mosby

Mud Volcano off Norway. Here, elevated fluid temperatures of up to 26 °C inhibit gas hydrate formation near the flow conduit and hydrates accumulate at some distance from the conduit centre (Ginsburg et al., 1999; Kaul et al., 2006).

On the northern slope of the GoM, 80% of the sediments containing gas hydrates are related to fluid flow focused along fault zones generated by salt tectonics (Milkov and Sassen, 2001) and the low permeability of the clay-rich sediments above the salt diapirs (Reilly et al., 1996). Thus, variations in in situ  $CH_4$  concentrations are also related to this brine advection and have an important impact on the methane budget of the Gulf of Mexico, as was also pointed out by Ruppel et al. (2005). However, due to the different origins and pathways of the advecting fluids (Reitz et al., 2007) there is no direct correlation between the advection rates and the chlorinity in shallow sediments. At GC415, a low chlorinity enables the occurrence of gas hydrates in MAC-04, although a shallow AOM zone indicated a very high advection rate. DAPC-04 (GC415), however, is characterized by lower advection rates but high chlorinity and a lower  $CH_4$  concentration in the presence free gas only. At GC185, DAPC-01 originates from a site with a similar advection rate but is low in chlorinity and allows gas hydrate formation. Here  $CH_4$  concentrations are high. This suggests

that in the Gulf of Mexico the chlorinity is the most important control on the CH<sub>4</sub> concentrations in these areas of high advection.

Our observations possibly suggest a highly dynamic gas hydrate/free gas system in the shallow sediments of the vent sites caused by frequent temperature, and possibly salinity, changes. MacDonald et al. (1994) noted that bottom water temperatures change between 6 and 11 °C over short time periods at the shallow GC185 seep site. These temperature changes significantly alter the depth of the lower boundary of the GHSZ (Fig. 10). At 11 °C gas hydrates would not be stable at any depth whereas at 6 °C the boundary would shift below the AOM zone in MAC-07 and methane could be stored in gas hydrates. Changes of the advection rate would have similar effects as will the occurrence of crude oil that was present in considerable amounts at GC415. Crude oil and C<sub>6</sub>-hydrocarbons induce large pressure depressions in gas hydrate stability (Sloan, 1998; Hara et al., 2005 and references therein).

### 5.5. Gas hydrate volume

The gas hydrate volumes from the pressure cores are the first values based on in situ methane concentrations in shallow seep site sediments. At sites where gas hydrates are present, their volume ranges between 8 and 13% of the core volume. These values are well within the average hydrate occupancy of 5–15% of sediment volume in high fluid flow sites (Milkov, 2005) although this average is not specific to shallow and deep sediments. Gas hydrate volumes previously determined in shallow sediments of seep sites vary between 1.2% on average (Ginsburg et al., 1999) and up to 60% in some parts of the cores (Schmidt et al., 2005). A comparison between these values is impossible since they all refer to different sediment volumes. The only other quantification of gas hydrates in the shallow sediments on the Louisiana Slope originates from a regional investigation (59,000 km<sup>2</sup>) on a large number of conventional gravity cores (Milkov and Sassen, 2001). The authors estimated gas hydrates to account for 0.5%cv of the shallow sediments in the overall area, assuming seawater salinity of 35. A study of the Håkon Mosby Mud Volcano seep sites (Ginsburg et al., 1999) allows for a better comparison with our data. Here, visual observations and chloride measurements indicate that volumes near the seep centre reach 25%cv. Overall the authors calculated a ratio of 1.2%cv for the shallow sediments of the mud volcano. It is clear that gas hydrate volumes at seep sites are still a considerable unknown, even without considering the low accuracy of most methods. The pressure cores give both a high ac-

curacy and are easy to use, greatly improving the data base for shallow sediments.

### 5.6. Gas hydrate composition

A variety of investigations have focused on gas hydrate compositions in the Gulf of Mexico (Brooks et al., 1984; Sassen et al., 1999; MacDonald et al., 2003). The reported compositions and standard deviations reported from GC185 (Sassen et al., 1999; Chen and Cathles, 2003) are within the range of those found during the SO174 campaign. In comparison, the data from cruise SO174 show slightly lower C<sub>1</sub> (4%) compositions at GC185 whereas C<sub>2</sub> and C<sub>3</sub> are somewhat higher on average and vary considerably between the sites. At these shallow sites this is of major importance for the stability of the gas hydrate (Fig. 10; TVG-10 and GC-02). At the deeper site GC415, a mixture of structure I and II gas hydrate were seen (Kuhns, Univ. of Göttingen, Germany, personal communication, 2005), but no pure sI gas hydrate could be detected via pressure coring. Two cores from GC415 (MAC-12 and DAPC-3) had CH<sub>4</sub> compositions of >99 vol.%, although, they did not exceed C<sub>eq</sub>. The major areas of gas hydrate formation seem to be related to the advection of deep ‘thermogenic’ hydrocarbons. Due to the high supply of C<sub>2+</sub> and variable composition of the natural gas hydrates, the stability field in the Green Canyon area varies considerably.

## 6. Conclusions

The deployment of two new pressure-coring devices, the Multi-Autoclave-Corer (MAC) and the Dynamic Autoclave Piston Corer (DAPC) was very successful. For the first time, they enable the retrieval of pressurized near-surface sediment cores of up to 2 m length and allowed the measurement of in situ methane concentrations and gas hydrate budgets. The methane concentrations exceeded conventional ex situ concentrations and calculated equilibrium concentrations up to two orders of magnitude, emphasizing the necessity of pressurized coring to determine the complexity of focused fluid flow systems. A sub-sampling possibility of the pressure cores and a complex investigation of the cores for physical properties and with CT, could further enhance the quality of the data.

Focused gas and brine advection create a complex distribution of free and hydrate-bound methane within single seep sites. The elevated salinity often related to the focused fluid flow in the Gulf of Mexico can shift the lower boundary of GHSZ to sediment depths of the AOM zone where methane concentrations are not

sufficient for gas hydrate formation because of microbial oxidation of methane. Below the GHSZ, excess methane is present as free gas. This can lead to a decrease in methane concentrations by one order of magnitude in areas of highest fluid flow and an elevated escape of methane from the sediment. Small changes in parameters determining the gas hydrate stability can considerably alter these conditions across the AOM zone, increasing the short term variability of the system. The alteration of gas hydrate systems by brine flow is particularly important in the focused fluid flow that is widespread along continental margin affected by halokinesis, such as the Gulf of Mexico (Sager et al., 2003) or offshore Angola (Tari et al., 2003).

### Acknowledgement

We greatly appreciate the support at sea by the masters and crews of R/V SONNE, A. Petersen and E. Anders and sincerely thank M. Pieper for the excellent construction of the degassing tool. Thanks to C. Gräf for her grand work with the CT scanner, V. Blinova, X. Han, L. Hmelo, and S. Kriwanek for their support in the pore water analysis, D. Masson for proof reading and to the anonymous reviewer. We thank G. Dickens for the many constructive comments and suggestions in his review. Financial support for the OMEGA project was granted within the GEOTECHNOLOGIEN program of the BMBF (FKZ 03G0566A) and the Deutsche Forschungsgemeinschaft as part of the DFG-Research Center Ocean Margins. This is publication GEOTECH-230 of the GEOTECHNOLOGIEN program and RCOM publication No 0543.

### References

- Abegg, F., Freitag, F., Bohrmann, G., Brueckmann, W., Eisenhauer, A., Amann, H., Hohnberg, H.J., 2003. Free gas bubbles in the hydrate stability zone: evidence from CT investigation under in situ conditions. EUG/AGU Meeting, Nice, France, Abstract #EAE-A-10342.
- Abegg, F., Hohnberg, H.J., Bohrmann, G., Freitag, J., under revision. Development and application of pressure core sampling systems for the investigation of gas and gas hydrate bearing sediments, Deep Sea Research, Part I.
- Archer, D., Buffett, B.A., 2005. Time-dependent response of the global ocean clathrate reservoir to climatic and anthropogenic forcing. *Geochemistry Geophysics Geosystems* 6, Q03002.
- Bangs, N.L.B., Sawyer, D.S., Golovchenko, X., 1993. Free gas at the base of the gas hydrate zone in the vicinity of the Chile triple junction. *Geology* 21 (10), 905–908.
- Bernard, B.B., Brooks, J.M., Sackett, W.M., 1976. Natural gas seepage in the Gulf of Mexico. *Earth and Planetary Science Letters* 31, 48–54.
- Bernard, B.B., 1979. Methane in marine sediments. *Deep-Sea Research* 26 A, 429–443.
- Bohrmann, G., Schenck, S., 2004. RV SONNE cruise report SO174: OTEGA II. GEOMAR Report, vol. 117. IFM-GEOMAR, Kiel, Germany.
- Brooks, J.M., Kennicutt II, M.C., Fay, R.R., McDonald, T.J., 1984. Thermogenic gas hydrates in the Gulf of Mexico. *Science* 225, 409–411.
- Buffett, B.A., Archer, D., 2004. Global inventory of methane clathrate: sensitivity to changes in the deep ocean. *Earth and Planetary Science Letters* 227, 185–199.
- Chen, D.F., Cathles III, L.M., 2003. A kinetic model for the pattern and amounts of hydrate precipitated from a gas steam: application to the Bush Hill vent site, Green Canyon Block 185, Gulf of Mexico. *Journal of Geophysical Research* 108 (B1), 2058, doi:10.1029/2001JB001597.
- Dickens, G.R., 2001. The potential volume of oceanic methane hydrates with variable external conditions. *Organic Geochemistry* 32, 1179–1193.
- Dickens, G.R., Paull, C.K., Wallace, P., ODP Leg 164 Scientific Party, 1997. Direct measurement of in situ methane quantities in a large gas-hydrate reservoir. *Nature* 385, 426–428.
- Dickens, G.R., Wallace, P.J., Paull, C.K., Borowski, W.S., 2000. Detection of methane gas hydrate in the pressure core sampler (PCS): volume–pressure–time relations during controlled degassing experiments. In: Paull, C.K., Wallace, P.J., Dillon, W.P. (Eds.), *Proceedings of the Ocean Drilling Program, Scientific Results*. Ocean Drilling Program, College Station, TX, pp. 113–126.
- Fu, B., Aharon, P., 1998. Sources of hydrocarbon-rich fluids advecting on the seafloor in the northern Gulf of Mexico. *Transactions — Gulf Coast Association of Geological Societies* 48, 73–82.
- Ginsburg, G.D., Milkov, A.V., Soloviev, V.A., Egorov, A.V., Cherkashev, G.A., Vogt, P.R., Crane, K., Lorenson, T.D., Khutorskoy, M.D., 1999. Gas hydrate accumulation at the Håkon Mosby Mud Volcano. *Geo-Marine Letters* 19, 57–67.
- Haeckel, M., Suess, E., Wallmann, K., Rickert, D., 2004. Rising methane gas bubbles from massive hydrate layers at the seafloor. *Geochimica et Cosmochimica Acta* 68 (21), 4335–4345.
- Hara, T., Hashimoto, S., Sugahara, T., Ohgaki, K., 2005. Large pressure depression of methane hydrate by adding 1,1-dimethylcyclohexane. *Chemical Engineering Science* 60 (11), 3117–3119.
- Heeschen, K.U., Dählmann, A., Hohnberg, H.J., Lykousis, V., Perissoratis, C., De Lange, G.J., Amann, H., Bohrmann, G., 2006. Pressurized near-surface sediment cores of Anaximander mud volcanoes, Eastern Mediterranean. EGU General Assembly, Geophysical Research Abstracts, 8, SRef-ID: 1607-7962/gra/EGU06-A-07005, Vienna, Austria.
- Holbrook, W.S., Hoskin, H., Wood, W.T., Stephen, R.A., Lizarralde, D., ODP Leg 164 Science Party, 1996. Methane hydrate and free gas on the Blake Ridge from vertical seismic profiling. *Science* 273, 1840–1843.
- Humphris, C.C., 1979. Salt movement in continental slope, northern Gulf of Mexico. *AAPG Bulletin* 63, 782–798.
- Hunt, J.M., 1979. *Petroleum Geochemistry and Geology*. W.H. Freeman, San Francisco.
- Iversen, N., Jørgensen, B.B., 1985. Anaerobic methane oxidation rates at the sulfate–methane transition in marine sediments from Kattégat and Skagerrak (Denmark). *Limnology and Oceanography* 30 (5), 944–955.
- James, A.T., Burns, B.J., 1984. Microbial alteration of subsurface natural gas accumulation. *The American Association of Petroleum Geologists Bulletin* 68 (8), 957–960.

- Johnson, B.D., Boudreau, B.P., Gardiner, B.S., Maass, R., 2002. Mechanical response of sediments to bubble growth. *Marine Geology* 187 (3–4), 347–363.
- Joye, S.B., 2004. The anaerobic oxidation of methane and sulfate reduction in sediments from Gulf of Mexico cold seeps. *Chemical Geology* 205, 219–238.
- Judd, A., 2002. The rising influence of shallow gas: an introduction to the Bologna Conference on “Gas in marine sediments”. *Continental Shelf Research* 22, 2267–2271.
- Kaul, N., Foucher, J.-P., Heesemann, M., 2006. Estimating mud expulsion rates from temperature measurements on Håkon Mosby mud volcano, SW Barents Sea. *Marine Geology* 229, 1–14.
- Kennicutt II, M.C., Brooks, J.M., Denoux, G.J., 1988. Leakage of deep, reservoirized petroleum to the near surface on the Gulf of Mexico continental slope. *Marine Chemistry* 24, 39–59.
- Krüger, M., Treude, T., Wolters, H., Nauhaus, K., Boetius, A., 2005. Microbial methane turnover in different marine habitats. *Palaeogeography, Palaeoclimatology, Palaeoecology* 12005, 6–17.
- Kvenvolden, K.A., Barnard, L.A., Cameron, D.H., 1983. Pressure core barrel: application to the study of gas hydrates, deep sea drilling project site 533, Leg 76. In: Sheridan, R.E., Gradstein, F.M., et al. (Eds.), *Initial Reports DSDP 76*. U.S. Govt. Printing Office, Washington, pp. 367–375.
- Kvenvolden, K.A., 1988. Methane hydrate — a major reservoir of carbon in the shallow geosphere. *Chemical Geology* 71 (1–3), 14–51.
- Kvenvolden, K.A., 1993. Gas hydrates — geological perspective and global change. *Reviews of Geophysics* 31 (2), 173–187.
- Kvenvolden, K.A., 1999. Potential effects of gas hydrate on human welfare. *Proceedings of the National Academy of Sciences of the United States of America* 96, 3420–3426.
- Lu, H., Matsumoto, R., 2005. Experimental studies on the possible influences of composition changes of pore water on the stability conditions of methane hydrate in marine sediments. *Marine Chemistry* 93, 149–157.
- MacDonald, I.R., Boland, G.S., Baker, J.S., Brooks, J.M., Kennicutt II, M.C., Bidigare, R.R., 1989. Gulf of Mexico chemosynthetic communities II: spatial distribution of seep organisms and hydrocarbons at Bush Hill. *Marine Biology* 101, 235–247.
- MacDonald, I.R., Guinasso, N.L., Sassen, R., Brooks, J.M., Lee, L., Scott, K.T., 1994. Gas hydrate that breaches the sea floor on the continental slope of the Gulf of Mexico. *Geology* 22, 699–702.
- MacDonald, I.R., Reilly, J.F., Best, S.E., Venkataramaiah, R., Sassen, R., Guinasso Jr, N.L., Amos, J., 1996. Remote sensing inventory of active oil seeps and chemosynthetic communities in the northern Gulf of Mexico. In: Schumacher, D., Abrams, M.A. (Eds.), *Hydrocarbon Migration and its Near-Surface Expression*. AAPG Memoir, pp. 27–37.
- MacDonald, I.R., Sager, W.W., Peccini, M.B., 2003. Gas hydrate and chemosynthetic biota in mounded bathymetry at mid-slope hydrocarbon seeps: northern Gulf of Mexico. *Marine Geology* 198, 133–158.
- Mango, F.D., 1997. The light hydrocarbons in petroleum: a critical review. *Organic Geochemistry* 26, 417–440.
- Martens, C.S., Chanton, J.P., Paull, C.K., 1991. Biogenic methane from abyssal brine seeps at the base of the Florida escarpment. *Geology* 19, 851–854.
- Milkov, A.V., 2004. Global estimates of hydrate-bound gas in marine sediments: how much is really out there? *Earth-Science Reviews* 66 (3–4), 183–197.
- Milkov, A.V., 2005. Molecular and stable isotope compositions of natural gas hydrates: a revised global dataset and basic interpretations in the context of geological settings. *Organic Geochemistry* 36 (5), 681–702.
- Milkov, A.V., Sassen, R., 2001. Estimate of gas hydrate resource, northwestern Gulf of Mexico continental slope. *Marine Geology* 179, 71–83.
- Milkov, A.V., Claypool, G.E., Lee, Y.-J., Xu, W., Dickens, G.D., Borowski, W.S., ODP Leg 204 Scientific Party, 2003. In situ methane concentrations at Hydrate Ridge, offshore Oregon: new constraints on the global gas hydrate inventory from an active margin. *Geology* 31 (10), 833–836.
- Milkov, A.V., Dickens, G.R., Claypool, G.E., Lee, Y.J., Borowski, W.S., Torres, M.E., Xu, W., Tomaru, H., Tréhu, A.M., Schultheiss, P., 2004. Co-existence of gas hydrate, free gas, and brine within the regional gas hydrate stability zone at Hydrate Ridge (Oregon margin): evidence from prolonged degassing of a pressurized core. *Earth and Planetary Science Letters* 222, 829–843.
- Orcutt, B.N., Boetius, A., Elvert, M., Samarkin, V.A., Joye, S.B., 2005. Molecular biogeochemistry of sulfate reduction, methanogenesis and the anaerobic oxidation of methane at Gulf of Mexico cold seeps. *Geochimica et Cosmochimica Acta* 69 (17), 4267–4281.
- Paull, C.K., Matsumoto, R., Wallace, P.J., 1996. *Proceedings of the Ocean Drilling Program Initial Reports* 164 620 pp.
- Paull, C.K., Ussler III, W., 2001. History and significance of gas sampling during DSDP and ODP drilling associated with gas hydrates. In: Paull, C.K., Dillon, W.P. (Eds.), *Natural Gas Hydrates: Occurrence, Distribution and Detection*. Am. Geophys. Union, Washington, DC, pp. 53–65.
- Paull, C.K., Ussler III, W., Lorenson, T.D., Winters, W., Dougherty, J., 2005. Geochemical constraints on the distribution of gas hydrates in the Gulf of Mexico. *Geo-Marine Letters*, doi:10.1007/s00367-005-0001-3.
- Reeburgh, W.S., 2003. Global methane biogeochemistry. In: Holland, H.D., Turekian, K.K. (Eds.), *Treatise on Geochemistry*. Elsevier, pp. 65–89.
- Reilly, J.F., MacDonald, I.R., Biegert, E.K., Brooks, J.M., 1996. Geologic controls and the distribution of chemosynthetic communities in the Gulf of Mexico. In: Schumacher, D., Abrams, M.A. (Eds.), *Hydrocarbon Migration and Its Near-Surface Expressions*. AAPG, Tulsa, USA, pp. 39–62.
- Reitz, A., Haeckel, M., Wallmann, K., Hensen, C., Heeschen, K.U., 2007. Origin of salt-enriched pore fluids in the northern Gulf of Mexico. *Earth and Planetary Science Letters* 259, 266–282.
- Roberts, H.H., Aharon, P., 1994. Hydrocarbon-derived carbonate buildups of the northern Gulf of Mexico continental slope — a review of submersible investigations. *Geo-Marine Letters* 14 (2–3), 135–148.
- Roberts, H.H., Carney, R.S., 1997. Evidence of episodic fluid, gas and sediment venting on the northern Gulf of Mexico continental slope. *Economic Geology* 92, 863–879.
- Rowan, M.G., Jackson, M.P.A., Trudgill, B.D., 1999. Salt-related fault families and fault welds in the northern Gulf of Mexico. *AAPG Bulletin* 83, 1454–1484.
- Ruppel, C., Dickens, G.R., Castellini, D.G., Gilhooly, W., Lizarralde, D., 2005. Heat and salt inhibition of gas hydrate formation in the northern Gulf of Mexico. *Geophysical Research Letters* 32 (L04605), doi:10.1029/2004GL021909.
- Sager, W.W., MacDonald, I.R., Hou, R., 2003. Geophysical signatures of mud mounds at hydrocarbon seeps on the Louisiana continental slope, northern Gulf of Mexico. *Marine Geology* 198, 97–132.
- Sahling, H., Rickert, D., Lee, R.W., Linke, P., Suess, E., 2002. Macrofaunal community structure and sulfide flux at gas hydrate deposits from the Cascadia convergent margin, NE Pacific. *Marine Ecology. Progress Series* 231, 121–138.
- Sassen, R., Joye, S., Sweet, S.T., DeFreitas, D.A., Milkov, A.V., MacDonald, I.R., 1999. Thermogenic gas hydrates and hydrocarbon

- gases in complex chemosynthetic communities, Gulf of Mexico continental slope. *Organic Geochemistry* 30, 485–497.
- Sassen, R., Losh, S.L., Cathles III, L., Roberts, H.H., Whelan, J.K., Milkov, A.V., Sweet, S.T., DeFreitas, D.A., 2001. Massive vein-filling gas hydrates: relation to ongoing gas migration from the deep subsurface in the Gulf of Mexico. *Marine and Petroleum Geology* 18, 551–560.
- Sassen, R., MacDonald, I., Requejo, A., Guinasso, N., Kennicutt II, M., Sweet, S., Brooks, J., 1994. Organic geochemistry of sediments from chemosynthetic communities, Gulf of Mexico slope. *Geo-Marine Letters* 14, 110–119.
- Schmidt, M., Hensen, C., Mörz, T., Müller, C., Grevemeyer, I., Wallmann, K., Mau, S., Kaul, N., 2005. Methane hydrate accumulation in “Mound 11” mud volcano, Coast Rica forearc. *Marine Geology* 216, 83–100.
- Sloan, E.D., 1998. *Clathrate Hydrates of Natural Gases*. Marcel Dekker, New York. 705 pp.
- Sloan, E.D., 2003. Fundamental principles and applications of natural gas hydrates. *Nature* 426, 353–359.
- Stadnitskaia, A., Ivanov, M.K., Blinova, V., Kreulen, R., Van Weering, T.C.E., 2006. Molecular and carbon isotopic variability of hydrocarbon gases from mud volcanoes in the Gulf of Cadiz, NE Atlantic. *Marine and Petroleum Geology* 23, 281–296.
- Suess, E., Torres, M.E., Bohrmann, G., Collier, R.W., Greinert, J., Linke, P., Rehder, G., Tréhu, A.M., Wallmann, K., Winckler, G., Zuleger, E., 1999. Gas hydrate destabilization: enhanced dewatering, benthic material turnover and large methane plumes at the Cascadia convergent margin. *Earth and Planetary Science Letters* 170, 1–15.
- Tari, G., Molnar, J., Ashton, P., 2003. Examples of salt tectonics from West Africa: a comparative approach. In: Arthur, T.J., MacGregor, D.S., Cameron, N.R. (Eds.), *Petroleum geology of Africa: new themes and developing technologies*. Special Publications. The Geological Society of London, London, 207, pp. 85–104.
- Thompson, K.F.M., 1996. Postulated generation of bacterial methane from seepage petroleum in sea floor sediments of the Gulf of Mexico. In: Schumacher, D., Abrams, M.A. (Eds.), *Hydrocarbon Migration and its Near-Surface Expression*. AAPG, Tulsa, pp. 331–334.
- Tishchenko, P., Hensen, C., Wallmann, K., Wong, C.S., 2005. Calculation of the stability and solubility of methane hydrate in seawater. *Chemical Geology* 219, 37–52.
- Tréhu, A.M., Bohrmann, G., Rack, F.R., Torres, M.E., 2003. Proceedings ODP Initial Reports, 204. Available from: [http://www.odp.tamu.edu/publications/204\\_IR/204ir.htm](http://www.odp.tamu.edu/publications/204_IR/204ir.htm). (cited 2004-01-20).
- Tréhu, A.M., Long, P.E., Torres, M.E., Bohrmann, G., Rack, R.R., Collett, T.S., Goldberg, D.S., Milkov, A.V., Riedel, M., Schultheiss, P., Bangs, N.L., Barr, S.R., Borowski, W.S., Claypool, G.E., Delwiche, M.E., Dickens, G.R., Gracia, E., Guerin, G., Holland, M., Johnson, J.E., Lee, Y.J., Liu, C.-S., Teichert, B.M.A., Tomaru, H., Vanneste, M., Watanabe, M., Weinberger, J.L., 2004. Three-dimensional distribution of gas hydrate beneath southern Hydrate Ridge: constraints from ODP Leg 204. *Earth and Planetary Science Letters* 222, 845–862.
- Weimer, P., Rowan, M.G., McBride, B.C., Kligfield, R., 1998. Evaluating the petroleum systems of the Northern Deep Gulf of Mexico through integrated basin analysis: an overview. *AAPG Bulletin* 82, 865–877.
- Worrall, D.M., Snelson, S., 1989. Evolution of the northern Gulf of Mexico, with emphasis on Cenozoic growth faulting and the role of salt. In: Bally, A.W., Palmer, A.R. (Eds.), *The Geology of North America*. Geological Society of America, Boulder, pp. 97–138.